Amplitude subtraction of color images by grating encoding

GUSTAVO RODRÍGUEZ-ZURITA AND JOSÉ F. VÁZQUEZ-CASTILLO
Colegio de Física, Escuela de Ciencias Físico-Matemáticas
Universidad Autónoma de Puebla
Apartado postal 1152, 72000 Puebla, Pue, México

Recibido el 2 de diciembre de 1992; aceptado el 28 de enero de 1993

ABSTRACT. The possibility of an extension of optical image subtraction to the case of color images is presented. Some related chromatic effects are also discussed by assuming the images as composed of color stimuli. Experimental results by using the Pennington's technique with a reflecting Ronchi ruling and polychromatic partially-coherent illumination are shown.

RESUMEN. Se plantea la generalización del método de substracción óptica de imágenes al caso en que éstas son coloreadas. Considerándolas como compuestas de estímulos cromáticos, se discuten algunos de los posibles efectos implicados por nuestra variante y se muestran resultados experimentales empleando la técnica de Pennington con rejillas de Ronchi reflectoras e iluminación policromática parcialmente coherente.

PACS: 42.30.Va; 42.80.Fn; 07.60.Dq

1. INTRODUCTION

Color image operations such as color image correlation techniques have been already proposed both optically [1, 2] and by computer methods [3, 4] for color image processing and color pattern recognition. Optical image subtraction is a related technique to extract differences between similar scenes and recently, an analysis of color image subtraction by achromatic diffraction was carried out [5]. Optical image subtraction was proposed long ago to extract intensity differences between two gray-tone images by using the Herschel effect [6] or fluorescent screens [7] among other phenomena suitable as the basis to perform mathematical operations optically on images illuminated with incoherent light [8]. However, soon after the development of laser light, subtraction of the amplitudes of two gray-tone transparencies became a reliable technique easily accomplished by introducing a phase shift of π radians between them under coherent illumination. This phase shift can be done by a variety of ways, but many of them can be collected into one of two groups: whether interferometric methods or grating encoding methods [9]. Because several grating methods can still have good performance with polychromatic partially-coherent light [10, 11], their use gave rise later to color-related applications such as subtraction of gray-tone images by colorimetric measurements [12, 13] and pseudocolor image-difference detection [14-16]. In addition, some of these techniques may be employed for color image subtraction as well [11]. Although a description of simple filtering of color images are to

be found in the literature (see Ref. [17], for example), a study of the particular chromatic effects that color image subtraction leads to are not available.

Within this context, early efforts to carry out image subtraction with white light sources does not pay full attention of the benefits which offers an encoding technique proposed by Pennington *et al.* and well established for coherent illumination [18]. A natural extension of the Pennington's technique to the case of having polychromatic partially-coherent illumination seems to be particularly suitable to optically perform color image subtraction [19]. Because some color operations which result from this technique can found applications in color instrumentation, color image processing, color pattern recognition and color metrology, it may be worthy to explore them. Along this work, chromatic effects appearing as consequence of the Pennington's technique are briefly discussed. Preliminary experimental results by encoding with a reflecting Ronchi ruling are also shown. Incidentally, the use of a reflecting ruling to achieve composite, interlaced images for image subtraction after the Pennington's technique is well known since first proposed by Dashiell *et al.* for gray-tone image difference applications [20].

2. COLOR IMAGE AMPLITUDE-SUBSTRACTION

Two color transparencies of real amplitude transmittances denoted by $O_f = O_f(\mathbf{r}, \lambda)$ and $O_g = O_g(\mathbf{r}, \lambda)$ are assumed such that

$$0 \leq O_f, \quad O_g \leq 1;$$

that is to say, each transparency produces no phase changes at all. Correspondingly, there are two object irradiance distributions which, in general, can be determined by $|O_f(\mathbf{r}, \lambda)|^2$ and $|O_g(\mathbf{r}, \lambda)|^2$. A colored slide f is supposed to be made up with colored points, each at position $\mathbf{r}$ and with tristimulus values (refered to the CIE 1931 system) given by

$$X_f(\mathbf{r}) = k \int_\lambda |O_f(\mathbf{r}, \lambda)|^2 S(\lambda) \bar{x}(\lambda)\, d\lambda, \tag{1.a}$$

$$Y_f(\mathbf{r}) = k \int_\lambda |O_f(\mathbf{r}, \lambda)|^2 S(\lambda) \bar{y}(\lambda)\, d\lambda, \tag{1.b}$$

$$Z_f(\mathbf{r}) = k \int_\lambda |O_f(\mathbf{r}, \lambda)|^2 S(\lambda) \bar{z}(\lambda)\, d\lambda, \tag{1.c}$$

and similarly for object g, where the spectral radiance transmittance associated to the particular point of position $\mathbf{r}$ is set equal to the value of its irradiance; $\bar{x}(\lambda)$, $\bar{y}(\lambda)$ and $\bar{z}(\lambda)$ are the color-matching functions of the standard colorimetric observer; $S(\lambda)$ is the spectral radiance distribution of a standard illuminant and

$$k = 100 / \int_\lambda S(\lambda) \bar{y}(\lambda)\, d\lambda = 100/V_s, \tag{2}$$

where the integral extends from $\lambda = 400$ nm to $\lambda = 700$ nm. Here, V_s denotes the luminance of the source computed in accordance with the luminous efficiency function $V(\lambda) \equiv \bar{y}(\lambda)$ [21].

Assuming an amplitude-subtraction operation performed with the objects f and g (by means of the Pennington's technique [18], for example), the new object has, as tristimulus values, the following ones:

$$X_\Delta(\mathbf{r}) = k \int_\lambda |O_f(\mathbf{r},\lambda) - O_g(\mathbf{r},\lambda)|^2 S(\lambda)\bar{x}(\lambda)\, d\lambda$$

$$= X_f + X_g - 2k \int_\lambda O_f O_g S(\lambda)\bar{x}(\lambda)\, d\lambda, \tag{3.a}$$

$$Y_\Delta(\mathbf{r}) = Y_f + Y_g - 2k \int_\lambda O_f O_g S(\lambda)\bar{y}(\lambda)\, d\lambda, \tag{3.b}$$

$$Z_\Delta(\mathbf{r}) = Z_f + Z_g - 2k \int_\lambda O_f O_g S(\lambda)\bar{z}(\lambda)\, d\lambda, \tag{3.c}$$

where the explicit dependance of the objects' distributions were dropped for simplicity. Interference between terms having close values of wavelength are neglected. Then, the pertinent CIE chromaticity coordinates (x_Δ, y_Δ) can be determined from above. By writing $X_i + Y_i + Z_i = V_i/Y_i$, where Y_i denotes the y chromaticity coordinate of object i and $i = f, g$, the results are

$$x_\Delta = \frac{x_f(V_f/y_f) + x_g(V_g/y_g) - 2k \int_\lambda O_f O_g S(\lambda)\bar{x}(\lambda)\, d\lambda}{V_f/y_f + V_g/y_g - 2k \int_\lambda O_f O_g S(\lambda)[\bar{x}(\lambda) + \bar{y}(\lambda) + \bar{z}(\lambda)]\, d\lambda}, \tag{4.a}$$

and

$$y_\Delta = \frac{y_f(V_f/y_f) + y_g(V_g/y_g) - 2k \int_\lambda O_f O_g S(\lambda)\bar{y}(\lambda)\, d\lambda}{V_f/y_f + V_g/y_g - 2k \int_\lambda O_f O_g S(\lambda)[\bar{x}(\lambda) + \bar{y}(\lambda) + \bar{z}(\lambda)]\, d\lambda}. \tag{4.a}$$

The role of the product $O_f O_g$ as integrand in the integrals of the chromaticity coordinates becomes clear, for if it were zero for all values of λ within the integration range, the expressions would reduce to the case of additive mixture of the stimuli with spectral radiances $|O_f|^2$ and $|O_g|^2$. Thus, for example, monochromatic stimuli do not contribute to the integrals of the color subtraction object's chromaticity coordinates. Such stimuli just mix additively.

For isoilluminat-stimuli, $V_f/y_f = V_g/y_g \equiv V/y$. Then, Eq. (4.$a$) reduces to

$$x_\Delta = \frac{x_f + x_g - \frac{2ky}{V} \int_\lambda O_f O_g S(\lambda)\bar{x}(\lambda)\, d\lambda}{2\left[1 - \frac{ky}{V} \int_\lambda O_f O_g S(\lambda)[\bar{x}(\lambda) + \bar{y}(\lambda) + \bar{z}(\lambda)]\, d\lambda\right]} \tag{5}$$

and a similar expression for y_Δ. The numerical difference of x_Δ and $(x_f + x_g)/2$ depends on the ratios of each integral containing the product $O_f O_g$ to the total radiant power of anyone of the two stimuli.

3. CHROMATIC EFFECTS

To visualize several chromatic effects, calculation of Eqs. (3) was carried out. For this purpose, approximations of integrals by summations were used with a wavelength interval $\Delta\lambda = 5$ nm. Tables of spectral tristimulus values CIE 1931 both for the standard colorimetric observer and for standard sources were taken from Ref. [22] from 380 nm to 780. Standard illuminant D_{65} was employed. Plots of chromaticity coordinates are shown in Fig. 1.

3.1. Color image subtraction

From the first equality of Eq. (3.*a*), it can be shown that

$$X_\Delta(\mathbf{r}) = k \int_\lambda |\Delta(\mathbf{r}, \lambda)|^2 S(\lambda)\, \mathbf{x}(\lambda) d\lambda, \tag{6}$$

with $|\Delta(\mathbf{r}, \lambda)| = |O_f(\mathbf{r}, \lambda) - O_g(\mathbf{r}, \lambda)|$ and similarly for the two remaining tristimulus values. Then, after subtraction operation the resulting stimulus is $|\Delta(\mathbf{r}, \lambda)|^2$. As examples of this case, hypothetical spectral transmittance distributions composed of a narrow-band spectral distribution centered at a particular wavelength added to an equal-energy spectral distribution were calculated and their respective chromaticity coordinates plotted and labeled from A to J as in Fig. (1.a). Adjacent distributions have overlapping regions. All of these spectral distributions but the one labeled as PIVOT (E) were subtracted from PIVOT according to Eq. (3.*a*), and the resulting chromaticity coordinates labeled in the same scheme from a to j respectively. Shifts of the original chromaticity coordinates in diverse amounts can be seen.

3.2. Contrast inversion and complementary colors

Contrast inversion is a well-known special application of image subtraction and it was extensivelly discussed in Ref. [23] for equal bar-width grating encoding in the coherent case under the name of "clear raster". For a given wavelength λ, the contrast of image $O_f(\mathbf{r}, \lambda)$ becomes inverted under subtraction operation when $O_g(r, \lambda) \equiv 1$. Then, subtraction of $O_f(\mathbf{r}, \lambda)$ and such an equal-energy stimulus results in

$$|\Delta(\mathbf{r}, \lambda)| = |O_f(\mathbf{r}, \lambda) - 1|. \tag{7}$$

If $O_f(\mathbf{r}, \lambda)$ is nearly an equal-energy stimulus of the same constant amplitude value, then $\Delta(\mathbf{r}, \lambda)$ tends to be black, whereas if $O_f(\mathbf{r}, \lambda)$ is nearly black, $\Delta(\mathbf{r}, \lambda)$ turns to be bright.

Another effect appears even if $|O_f(\mathbf{r}, \lambda)|^2$ has roughly the same total energy as the achromatic stimulus. Hypothetical color stimuli of approximately the same energy were

subject to the subtraction operation with an equal-energy stimulus. In this example, all the stimuli involved are practically isoiluminant. Their respective chromaticity coordinates are shown in Fig. 1.b, where it is possible to note that an original color (upper case labels) and its resulting subtraction (lower case labels) lie in opposite sides over the line joining them with the illuminant (D), as is the case for complementary colors.

3.3. Metameric stimuli

The spectral reflectance factors of three objects which for the CIE 1931 standard observer provide metameric stimuli when illuminated by CIE standard illuminant D_{65} [as given in Ref. [21], Table 2 (3.3.10)] were used as spectral transmittances. Simple interpolation of adjacent values to have $\Delta\lambda = 5$ nm was required. Its chromaticity coordinates are shown in Fig. 1.c with labels A, B and C. Results of the three mutual subtractions according to Eqs. (4) show very different color coordinates, thereby demonstrating the spectral dependance of the subtraction operation. Subtraction between each metameric stimulus and the illuminant D_{65} give close chromaticity coordinates which are labeled with ⟨dif.⟩.

3.4. Color enhancement

All of the same spectral distributions as in Sect. 3.1 were used again in Fig. 1.d. Image subtraction with each stimuli and an equal-energy stimulus (PIVOT) were performed and the resulting chromaticity coordinates plotted and labeled from a and j accordingly. Higher saturation for each stimuli is to be seen after subtraction. This effect is, of course, similar to the zero-order color processing for color enhancement as reported in Ref. [24].

4. EXPERIMENTAL RESULTS

To test the main conclusions, a reflecting Ronchi ruling was first made by means of photolithography and using a commercial Ronchi ruling ($\sim$ 300 lines/inch). This kind of rulings has typically dark bars wider as the clear ones, so that we got a reflecting ruling with reflecting stripes wider as the transparent ones. Both colored scenes and uniform color fields were encoded on commercial color slide film with the help of the reflecting grating [20] (Figs. 2.a or 2.b), so as to achieve the composite color slide consisting of interlaced stripes having samplings of a scene and a field alternatively (see, for example, Fig. 3.c) or interlaced samplings of two similar pictures. As fields, a white field and a green one were used. The total radiant power of each image to encode was balanced with a neutral density filter in order to achieve images with nearly equal average radiant power. After appropriate development, each composite image was placed on a telecentric, coherent optical image forming system for observing through a microscope at the system's image plane. The spectrum showed no missing orders as expected and contrast reversal was observed for each diffraction order but the zeroth, in agreement with Ref. [19]. To test the possibility of some color operations, each one of the color composite images was placed at the object plane of an optical, polychromatic partially-coherent image forming system. Results are shown in Fig. 3.

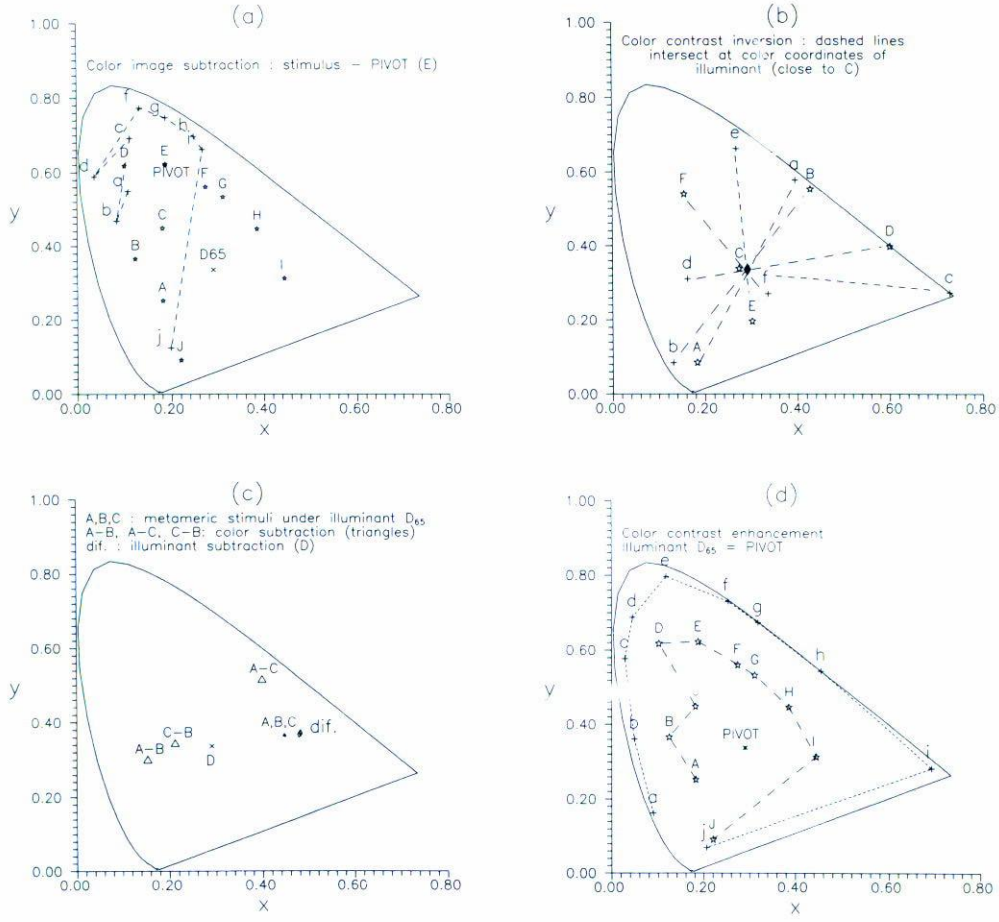

FIGURE 1. a) Color image subtraction. b) Color contrast inversion. c) Metameric colors. d) Color contrast enhancement.

Contrast inversion was achieved in Fig. 3.b within a region smaller than the whole original scene (Fig. 3.a). In that region a white, bright field was encoded. Fig. 3.c shows another similar scene encoded with a green field with an spatial frequency much smaller as in the previous case. After blocking out the zeroth order, changes of colors can be seen in Fig. 3.d. For example, the yellow region of the color chart clearly becomes red, a color shift similar to the one plotted in Fig. 1.a. However, the red original region becomes yellow. This could be explained as a case of additive mixture. Another two plausible effects are the violet-to-yellow shift of the girl's sweater and the white-to-magenta shift of the color chart's frame. Contrast reversal is also present in the chart's background and in the scene's background. Green regions of the chart become black.

Fig. 3.e shows the difference extracted from the encoding of two similar scenes. Codification was achieved with the setup of Fig. 2.a, which employs the same illuminant. High intensity borders reveal regions of no coincidence. The necklace around our model's neck was another difference (compare Figs. 3.a and 3.c). The bright white spots that spread

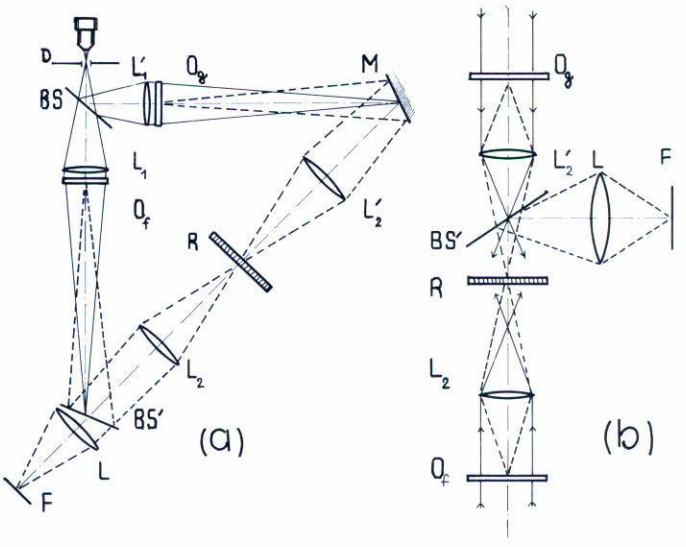

FIGURE 2. a) Experimental setup to make color composite images with a polychromatic light source. b) Experimental setup to make color composite images with two light sources [20]. D is a diagraphm at the focal plane of a microscope objective, BS and BS' are beam splitters. With L_1 and L_1' the color transparencies O_f and O_g are illuminated and then, imaged to the reflecting Ronchi ruling R by means of the lenses L_2 and L_2' through the beam splitter BS' and the mirror M. Lens L images R onto the film plane F.

intensity borders reveal regions of no coincidence. The necklace around our model's neck was another difference (compare Figs. 3.a and 3.c). The bright white spots that spread over the scene are due to diffracted light coming up from dust on the slide. Fig. 3.f is similar to the previous one, but encoding was achieved with the setup of Fig. 2.b, which uses two different illuminants. Regions over the face and the chest of the girl shows changes of colors and darkening, which precludes the possibility of being additive superposition. The necklace is again conspicuous.

The best chromatic effects were observed with low spatial frequencies of the interlaced images. This is due probably to the rather poor resolution of the film employed (400 ASA color slide film), as an inspection through the microscope suggests. Bubbles within the film substrate and film grain scattering were spected to cause phase alterations, but this effects, although present, do not hide the conclusions based only on diffraction theory of image formation. Different illuminants (Fig. 2.b) introduces its spectral radiance distributions. In this case, irradiance balance for the images under study has to take into account non-visible radiation. Real-time regime operation of the first setup seems to be possible by compensating undesirable phase differences as well as dispersion (Ref. [25]).

FIGURE 3. a) Typical test color slide. b) Obstruction of the zeroth diffraction order shows contrast reversal over certain region of a): interlacing of a white region, smaller than the test image size, was previously performed. c) Interlaced images of a green field and a color image. d) Image after obstruction of zeroth diffraction order: this image shows color shifts of c). e) Image subtraction of two similar color pictures showing displacement between them as bright edge lines. f) Image subtraction of two similar color scenes under different illuminants. ☛


PHOTO RESEARCH

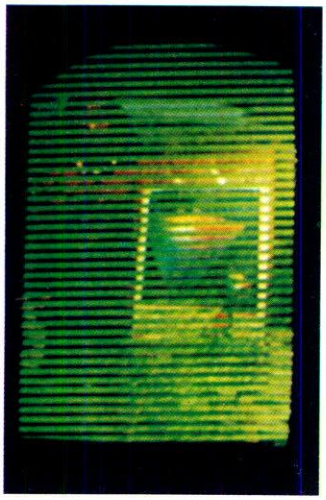

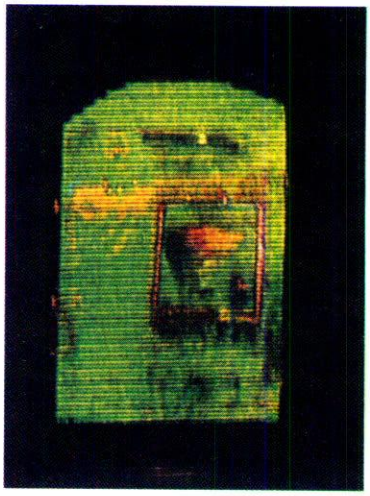

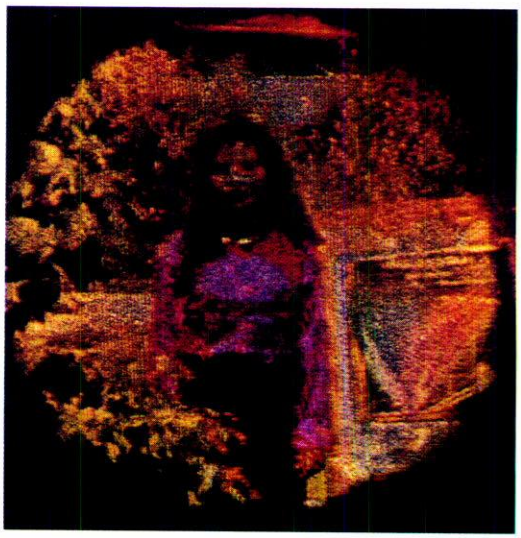

5. CONCLUSIONS

The technique described by Pennington *et al.* for image subtraction [18] was extended to color images and some of its chromatic effects were derived and discussed. Although the interlacing of color images and the whole technique can be implemented in a number of ways, experimental results with an optical setup using a polychromatic, partially-coherent source and commercial color slide film were shown, thereby demonstrating the feasibility of the variant. Besides, these chromatic effects should appear while processing color images with similar methods based also in amplitude subtraction under polychromatic illumination. The color effects suggest the usefulness of color image subtraction to the fields of colorimetry, color difference, metamerism, color enhancement and color image processing.

ACKNOWLEDGEMENTS

We gratefully acknowledge Javier Santamaria for enlightening lectures which introduced us to the field. We are indebted to J. de Jesus Pedraza-Contreras for his hints about the best way to achieve reflecting Ronchi rulings by using the techniques available and express sincere appreciation to Alberto Cordero-Davila for providing his own work's Ronchi rulings while standing at INAOE (Tonantzintla, Pue.). The slide development was done at the Colegio de Fisica's photographic laboratory (UAP). We warmly thank to Elisa Arias for her kind cooperation.

REFERENCES

1. V. Venkateswara Rao, C. Joenathan and R.S. Sirohi, *Opt. Commun.* **61**, 5 (1987) 313.
2. G.G. Mu, D.Q. Cheng and Z.Q. Wang, *Opt. Lett.* **13**, 6 (1988) 434.
3. E. Badiqué, Y. Komiya, N. Ohyama, J. Tsujiuchi and T. Honda, *Opt. Commun.* **61**, 3 (1987) 181.
4. E. Badiqué, Y. Komiya, N. Ohyama, J. Tsujiuchi and T. Honda, *Opt. Commun.* **68**, 2 (1988) 91.
5. C. Illueca, R. Ferrière and J.P. Goedgebuer, *J. of Mod. Opt.* **37**, 6 (1990) 1095.
6. D.H. Kelly, *J.O.S.A.* **51**, 10 (1961) 1095.
7. E.A. Trabka and P.G. Roetling, *J.O.S.A.* **54**, 10 (1964) 1242.
8. A. Lohmann, *Opt. Acta* **6**, 4 (1959) 319.
9. J.F. Ebersole, *Opt. Engineer.* **14**, 5 (1975) 436.
10. F.T.S. Yu, T.H. Chao and S.L. Zhuang, *Appl. Opt.* **19**, 12 (1980) 1887.
11. S.T. Wu and F.T.S Yu, *Appl. Opt.* **20**, 23 (1981) 4082.
12. G.G. Mu, C.K. Chiang and H.K. Liu, *Opt. Lett.* **6**, 8 (1981) 389.
13. D.Z. Zhao, C.K. Chiang and H.K. Liu, *Opt. Lett.* **6**, 10 (1981) 490.
14. D. Zhao and H.K. Liu, *Opt. Lett.* **8**, 2 (1983) 99.
15. Z.M. Li, P.J. Ding and W.B. Hu, *Opt. Commun.* **69**, 2 (1988) 117.
16. L.Z. Cai and T.H. Chao, *J. of Mod. Opt.* **37**, 6 (1990) 1127.
17. M.E. Zhabotinski and A.A. Lapides, *Opt. Lett.* **7**, 3 (1982) 142.
18. K.S. Pennington, P.M. Will and G.L. Shelton, *Opt. Commun.* **2**, 3 (1970) 113.
19. G. Rodríguez-Zurita, *Rev. Mex. Fís.* **38**, 3 (1992) 420.
20. S.R. Dashiell, A.W. Lohmann and J.D. Michaelson, *Opt. Commun.* **8**, 2 (1973) 105.

21. G. Wyszecki and W.S. Stiles, *Color science. Concepts and methods, quantitative data and formulae*, 2nd ed., Wiley, New York, (1982).
22. G. Wyszecki, "Colorimetry", Section 9, in *Handbook of Optics*, Walter G. Driscoll ed., McGraw-Hill Book Co., New York (1978).
23. C. Roychoudhuri and D. Malacara, *Appl. Opt.* **14**, 7 (1975) 1683.
24. J. Santamaria, A. Plaza and J. Bescós, *Opt. Commun.* **45**, 4 (1983) 244.
25. J.W. Goodman, *Introduction to Fourier Optics*, McGraw-Hill Book Co., New York (1968) 248.